Journal of Technology and Value Addition, Volume 3 (1), 2021: (1-18)

Research Article

Development of a Novel Dental Filling Using Hydroxyapatite Derived from Waste Oyster Shells

M.T.S. Uresha[1], H.M.J.C. Pitawala[1*], G.G.N. Thushari [2]

jcpitawala@yahoo.com

[1]Uva Wellassa University, Faculty of Applied Sciences, Passara road, Badulla, Sri Lanka
[2]Uva Wellassa University, Faculty of Animal Sciences and Export Agriculture, Passara road, Badulla, Sri Lanka

Abstract

Oysters are a widely popular sea food in the world. However, after consuming soft edible parts, shells are discarded as a biological waste material although they have high mineral value. The aim of the percent study is developing novel zinc phosphate dental cement (ZPDC) by adding hydroxyapatite (HA) derived from waste oyster shells as reinforcing filler. Shells of Crassostrea madrasensis oyster species was selected for the study. First, oyster shells were crushed, grinded and sieved (< 63µm) to obtain CaO. The $Ca(OH)_2$ precursor was prepared at room temperature by dissolving CaO in water. HA was synthesized using wet precipitation method and sintered at 800°C for 1 hour. X-ray florescence spectroscopy (XRF) was used to obtain the chemical composition of the raw oyster shells and Ca/P ration of synthesized HA. Our results showed that CaO (88.5%), SiO_2 (3.78%), and Fe_2O_3 (3.15%) are the major components in these oyster shells and calculated stoichiometric Ca/P ratio was 1.7. The average particle size of sintered HA was around 1518 nm. The properties of developed HA were compared with commercial HA using Fourier Transform Infrared spectroscopy (FTIR) and X-ray Diffraction (XRD). It was indicated that results of sintered HA are compatible with the results of commercial HA. The resulted HA powder was added into zinc phosphate dental cement powder mixture in seven different ratios (0%, 1%, 2%, 5%, 10%, 20%, 50%) and different specimens were fabricated. In addition, mechanical properties such as compressive strength (CS), diametral tensile strength (DTS) and elution properties of the prepared specimens were determined. Among studied samples 10% HA added zinc phosphate cement was showed the highest CS (66.85 MPa) and DTS (18.88 MPa) with lowest elution percentages in water and aqueous lactic acid solutions of pH 5 and 3 respectively. Finally, it can be concluded that Hydroxyapatite synthesized from Crassostrea madrasensis oyster shells is an alternative reinforcing filler to develop the dental cement based on Zinc Phosphate.

Keywords: *Zinc phospate dental cement, hydroxyapatite, Crassostrea madrasensis, oysters*

1. Introduction

Oysters are a popular sea food all over the world. People have been consuming them since the pre-stone age. However, from the total weight of an oyster, around 70-90% is shell and it is discarded after scraping the edible meat. In 2016, 438 billion tons of oysters were produced. The majority of the shells were unduly discarded, presenting a public health problem (Jamarun *et al*., 2015). In Korea about 300,000 tons of oyster shells are generated annually and their government has financed a project to increase recycling of this waste. If this waste has been left untreated for a long time, it can be a source of nasty smell as a consequence of the decay of flesh remnants attached to the oyster or the microbial decomposition of salts into gases such as NH_3, H_2S and amines (Kantharia *et al*., 2014). Currently, they only 30% of the shells are being recycled and use for cement production, poultry and fish feed, fertilizer production and as a food additive. Still the majority around 70% is discarded.

Being an island, Sri Lanka has several ideal natural oyster habitats in the coastal belt of the country. Among them most notable ones are Trincomalee bay, Tangall and Mirissa fisheries harbor, Puttlam and Muttuwaran lagoons. However, oyster farming is done in Sri Lanka in minor scale (Piyathilaka *et.al*., 2012) and small portion of waste oyster shells is being used for poultry feed preparation in Sri Lanka.

Oysters coming under the Genus, *Crassostrea* and *Saccostrea* are observed along the Indian and Sri Lankan coasts (Abdulrahman *et al.,* 2014). Among them four species are considered economically important including *Crassostrea madrasensis, Crassostrea gryphoides, Crassostrea rivularis* and *Saccostrea cucullata.* (Yoon *et al.,* 2003) *C.madrasensis* and *S.caulata* are edible oyster species cultured in Sri Lanka. *C. madrasensis,* is more popular among them and has been selected for this study.

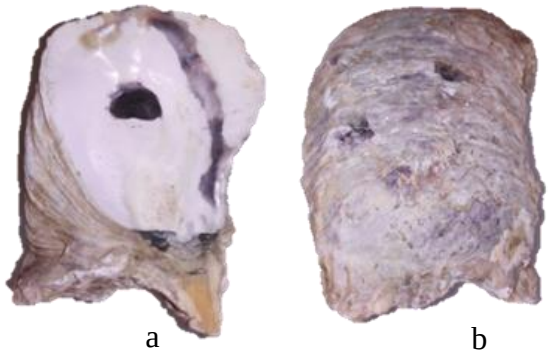

Figure 1: (a) Dorsal and (b) Ventral view of a cleaned *Crassostrea madrasensis* shell.

Hydroxyapatite (HA) is the main mineral constituent of human bones and teeth with the Ca/P molar ratio is 1.67. It is not only a biocompatible, non-toxic, non-immunogenic and non-inflammatory agent, but also bioactive (Wu *et al*., 2011). Synthesized HA can directly bond to the host bone and teeth as an artificial material. The main applications of HA are repairing defects in dental and orthopedic sites, immediate tooth replacement, augmentation of alveolar ridges, pulp capping material and maxillo-facial reconstruction, etc. Hence researchers have tried to customize its properties such as mechanical strength, solubility and sintering ability by controlling its composition, morphology and particle size (Wilcock *et al*., 2017).

The major component of an oyster shell is $CaCO_3$ and it is approximately around 96% and other components are in trivial amounts. Different methods such as wet chemical methods, hydrothermal processes, sol-gel synthesis and solid-state reaction have been adopted for the synthesis of HA from $CaCO_3$ sources like egg shells, lime stones, oyster shells (Rujitanapanich *et al*., 2014). However, the widely used technique is the wet precipitation method. Here, oyster shells are sintered to decompose $CaCO_3$ into CaO and dissolved in water to obtain $Ca(OH)_2$ precursor treated with H_3PO_4 to obtain HA.

A dental filling is a direct restoration that is used to repair a decayed or damaged tooth. There is a wide spectrum of dental fillings and out of them most popular types of dental fillings are metal fillings (gold, silver), amalgam fillings, composite resin fillings (chemically cured, light cured and dual cured), ceramic fillings and glass inomer fillings (acrylic resins). Among different ceramic fillings, zinc phosphate cement (ZPC) is one of the oldest dental cement and still it is being used in minor scale. The significance of the zinc phosphate dental cement in the modern world is that it acts as a standard to measure the properties of novel dental fillings (Fleming *et al*., 2001).

In this work, we developed a novel dental filling material based on zinc phosphate and hydroxyapatite (HA) derived from waste oyster shells. Waste shells of *Crassostrea madrasensis* oyster species was selected for the study. First, HA was synthesized and characterized for its chemical composition and structure. In addition, the properties of developed HA were compared with commercial HA. Finally, different zinc phosphate cement samples were prepared after incorporation of resulted HA powder and measured their mechanical properties.

2. Material and Methods

2.1 Synthesis of Hydroxyapatite

2.1.1 Preparation of CaO Powder

Raw waste oyster shells were obtained from "Tropical oysters" institute which is located at Nigambo, Sri Lanka. Shells were washed thoroughly with tap water and a brush and rinsed with distilled water. After that wet shells were dried in an oven at

120°C for two hours and grinded into a fine powder using a jaw crusher. Dry particles less than 63 µm were obtained using an auto sieve shaker (Matest, A060-01, Italy). Finally oyster shell powder was calcined in an electric muffle furnace (Nebertherm, Germany) at 900°C for one hour to obtain the CaO powder after releasing carbon dioxide.

2.1.2 Wet Precipitation of Hydroxyapatite

The resulted CaO powder (83.7 g) and distill water (510 ml) were added into a 1 l beaker and stirred continuously for 1 hour. Next the suspension was allowed to settle for five minutes and the supernatant was carefully separated from the sediment. The supernatant was the $Ca(OH)_2$ precursor and it was reacted with a solution of 40 ml orthophosphoric acid in 200 ml of distilled water. In order to obtain a hydroxyapatite slurry, phosphoric acid solution was added drop vice very slowly to $Ca(OH)_2$ precursor for three hours at room temperature (25°C) stirring vigorously. During the addition, the pH value was maintained between 8-10 to obtain the correct Ca/P stoichiometric ratio (1.67). Here, concentrated aqueous ammonia (NH_4OH) solution was used. Next the reaction mixture was allowed to age for 1 day and the precipitate was separated by vacuum filtration, washed twice with distill water. The filtered cake was oven dried at 120°C for four hours and then grounded to a powder using a mortar and pestle. Finally, resulted powder was sintered at 800°C for 1 hour.

2.2 Preparation of Ceramic Mixture

The composition of the prepared ceramic mixture (100 g) is shown in the following Table 1. Next the powder mixture was sintered at 1000°C for 1h and the sintered powder was grounded using a mortar and pestle.

Table 1: Composition of ceramic mixture

Compound	Weight ($\pm$ 0.01)/g
ZnO	90.20
MgO	8.20
SiO_2	1.40
Al_2O_3	0.12
CaF	0.08

2.3 Preparation of Liquid Mixture

The composition of the prepared liquid mixture (100 ml) is shown below in Table 2.

Table 2: Composition of the liquid mixture

Compound	Volume (± 0.1)/ml
H_3PO_4	48.0
Water	42.0

After preparing H_3PO_4 aqueous solution 3.0 g of Al powder and 7.0 g of Zn powder were added it. Special safety measures were taken since the reaction is exothermic and produce Hydrogen gas.

2.4 Preparation of HA added Ceramic Samples

Prepared HA was added into ceramic mixture in seven ratios (1%, 2%, 5%, 10%, 20%, 50%). For each sample, total weight was kept as 15 g. Table 3 shows the details of the prepared samples.

Table 3: Weight of hydroxyapatite in different samples

Weight %	HA weight (± 0.01)/g
0%	–
1%	0.15
2%	0.30
5%	0.75
10%	1.50
20%	3.00
50%	7.50

Samples from each ratio were prepared by carefully mixing powder mixture and liquid mixture on a clean dry cooled glass slab (placed in the refrigerator for 1 hour) using a stainless-steel spatula. In order to obtain a homogeneous consistency, the measured amount of powder was divided in to small portions and mixed with liquid one after the other.

The resultant pulp was deliberately inserted into a split wooden mold with cylindrical grooves (h=15 mm, d=12 mm) where the inside of the cavities was coated with wood wax. Next the samples were carefully removed from the mold after 24 hours.

2.5 Characterization

2.5.1 XRF Analysis

X-ray florescence spectrometer (Rigaku, Japan) was used to obtain the composition of the raw oyster shell powder and synthesized HA.

2.5.2 FTIR Analysis

Fourier Transform Infrared spectrophotometer (Bruker Alpha, Germany) was used to analyze the functional groups of the commercial HA, synthesized unsintered and sintered HA samples. It was carried out with the KBr pellet method in the frequency range of 500-4000 cm^{-1}.

2.5.3 XRD Analysis

Rigaku-Ultima IV X-Ray Diffractometer (KYOWAGLAS-XA^{TM}, Japan) was used to do the structural characterization of commercial HA, synthesized unsintered and sintered HA samples. X-Ray diffraction (XRD) patterns were collected by using Cu- kα = 1.5405 A° radiation.

2.5.4 Particle Size Analysis

Malvern Zetasizer version 7.03 (serial number: MAL1032006) particle size analyzer was used to analyze the particle size of synthesized sintered HA powder. Size distribution report by intensity and size statistic report by intensity were obtained.

2.5.5 Mechanical Characterization

The compressive strength (CS) and the diametral tensile strength (DTS) of the prepared samples were measured using the universal testing machine (JTMS1000, Taiwan). Diametral tensile strength (indirect tensile strength) is an indirect measurement of the tensile strength. There the cylindrical specimen is rolled and compressed as shown in the Figure 2.

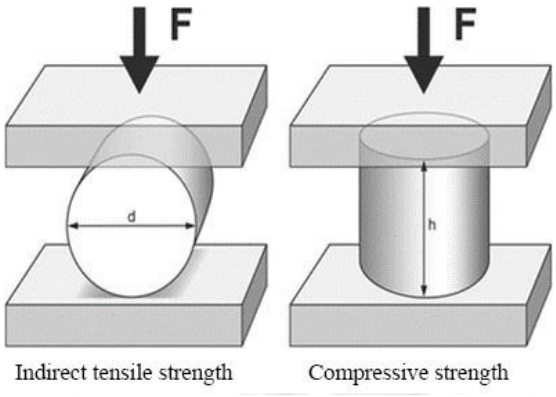

Figure 2: The schematic representation of DTS and CS

2.5.6 Elution Test

Elution is the loss of a desired material due an external factor with the passage of time. In the present work, elution properties of the Zinc phosphate dental cement were evaluated in water and aqueous lactic acid solutions of pH 3 and 5. A specimen from each ratio was taken and they were placed in an oven at 35°C for until a constant weight was obtained and it was recorded as the initial weight (m_0). After that they were immersed separately in McCartney bottles containing 15 ml from each solution and kept for seven days. Next the specimens were taken out and blotted with tissue paper and placed in the oven until a constant weight was obtained. It was recorded as dry weight (m_1), The elution percentage (E_p) was calculated using the following formula.

$$E_p = \frac{m_0 - m_1}{m_1} \text{ X } 100\% \quad (1)$$

3. Results and Discussion

3.1 XRF Analysis

3.1.1 Raw Oyster Shell Powder

The XRF analysis of raw oyster shells showed that it has CaO as the major constituent with 88.5%. Other oxides i.e., SiO_2 and Fe_2O_3 were the major impurities found in oyster shells containing 3.78% and 3.51% respectively. SiO_2 is a common impurity which found in clam, mussel oyster shells as they live in saline and brackish sandy bottoms. Fe_2O_3 is a result of poor water quality of lagoons, bays and the sea due to industrial pollutions. With the passage of time Fe_2O_3 and other impurities percent in the surrounding water accumulate in the valves of the oysters (Ragukumar *et al*., 1989). Biological metal accumulation by a wide variety of organisms, ranging from prokaryotes to eukaryotes, is a well-known phenomenon. These chemotrophic bacteria and algae colonized on top of the shell surface obtain

energy by the oxidation of electron donors in their environment. In some cases, reduced metals are used as an energy source, as in iron bacteria, or as electron donors or acceptors. In others, they are acted upon to detoxify the environment and precipitate the excess toxic metals or to concentrate iron for growth and eliminate competition (Murphy *et al*., 1976). Deposition of iron as ferric hydroxide in nodules and sheaths in species of green algae and in mucilaginous sheaths of freshwater cyanobacteria has been reported. Magnetite (Fe_3O_4) biomineralization by freshwater and marine magnetotactic and nonmagnetotactic anaerobic bacteria has also been investigated (Cariou *et al*., 2017).

Table 4: XRF results of raw oyster shell powder

Compound	Weight %
CaO	88.5%
SiO_2	3.78%
Fe_2O_3	3.51%
Al_2O_3	1.6%
MgO	0.628%

Al_2O_3 and MgO were found in trivial amounts as impurities. These results showed that certain purification steps are needed in order to obtain a highly purified $Ca(OH)_2$ precursor. Silicon dioxide and ferric oxide could easily be removed by gravity filtration as the sediment in the bottom of the container after magnetic stirring.

3.1.2 Synthesized Hydroxyapatite

XRF results of synthesized HA showed that CaO and P_2O_5 are in 53.6% and 42.8% respectively. In generally, the literal Ca/P of hydroxyapatite is 1.67. However, the calculated experimental stoichiometric Ca/P ratio of our synthesized HA was 1.709.The experimental value is very close to the theoretical value and it indicates that we can successfully synthesis hydroxyapatite following above procedure. A minor imbalance of synthesis product during high temperature treatment can lead to composition of β-, α-TCP, or other phases. One of the main non-stoichiometry reasons is inclusion of impurities, often substitutions of Ca^{2+} or interpenetration of other ions in the crystal lattice. In total, biological calcium phosphates are defined as calcium hydroxyapatites with deficient of calcium, $Ca_{10-x}(PO_4)_{6-x}(HPO_4)_x(OH)_{2-x}$ ($0<x<2$), including the substituting atoms or groups for example, Mg^{2+}, Na^+, K^+, Sr^{2+}, or Ba^{2+} substitute Ca^{2+}, CO_3^{2-}, H_2PO^{4-}, HPO_4^{2-}; SO_4^{2-} substitute PO_4^{3-}, F^-, Cl^-, CO_3^{2-} , and PO_4^{3-} substitute OH^- (Morgan *et al*., 2000).

3.2 FTIR Analysis

Figure 3 given below is the FTIR spectrum of commercial hydroxyapatite and Table 5 shows the wavenumbers of corresponding mode of assignments. Selected anion vibrations of PO_4^{3-} group *i.e*., P-O symmetric and asymmetric stretching can be found around wave numbers 560,600 and 960-1090 cm^{-1} having the highest intensity. Symmetric and asymmetric stretching vibrations of CO_3^{2-} group are appeared around 1418 and 1458 cm^{-1} with the small intensity values. The broad peak found in between 2500-3700 cm^{-1} with a medium intensity is due to the adsorbed water molecules (Reyes-Gasga *et al*., 2013).

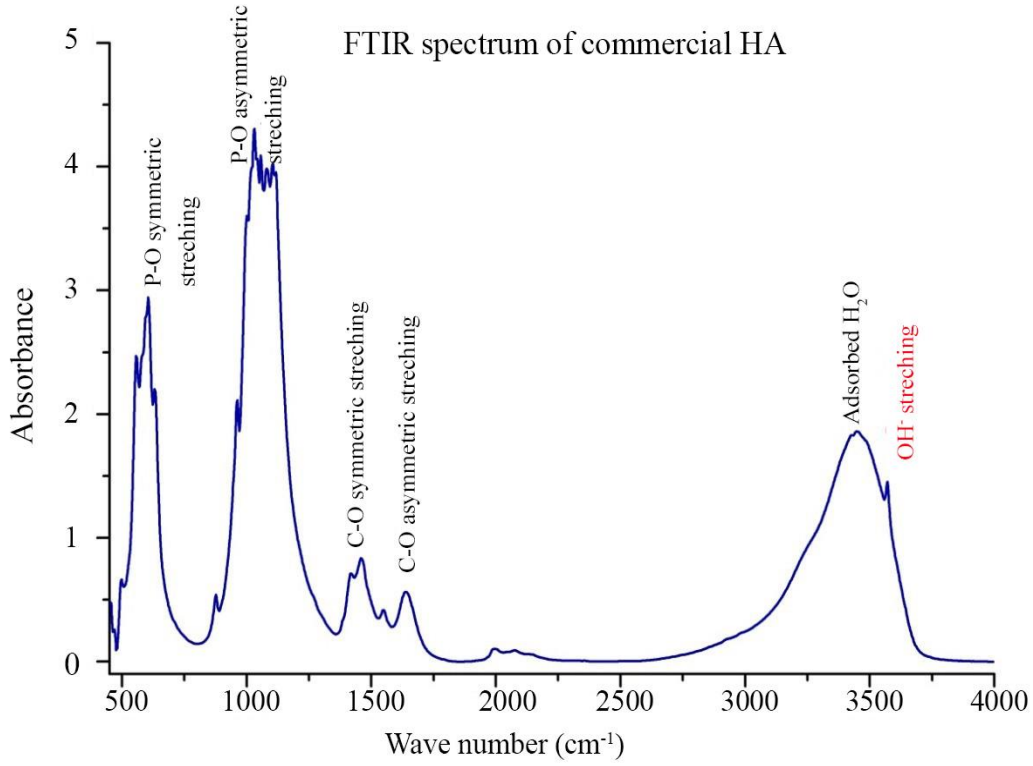

Figure 3: FTIR spectrum of commercial HA

Figure 4 shows the stacked FTIR spectrums of commercial, unsintered and sintered HA. It is clearly obvious that after sintering clarity of the peaks have increased and CO_3^{2-} and adsorbed water peaks have disappeared. The peak at 3572 cm^{-1} is due to the stretching mode of ionic OH^- which is crucial in conforming the structure of $Ca_5(PO_4)_3(OH)_2$ (Berzina-Cimdina and Borodajenco., 2012).

Table 5: Characteristic FTIR absorption bands of Hydroxyapatite

	Vibrational mode	Wave number (cm^{-1})
	P-O symmetric stretching	560, 600
PO_4^{3-}	P-O asymmetric stretching	960, 1039, 1090
	P-O bending	565
H_2O	adsorbed water	2500 – 3700
	O -H bending	1640
OH^-	vibration	630
	stretching	3572
HPO_4^{2-}	stretching	875
	C = O stretching	875
CO_3^{2-}	C – O symmetric stretching	1418
	C – O asymmetric stretching	1458

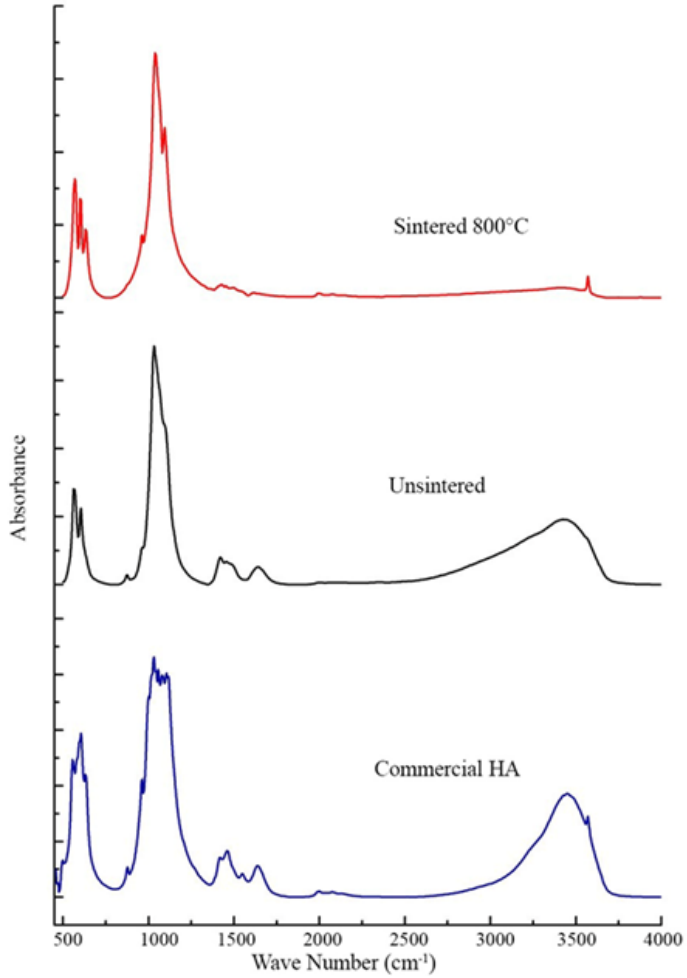

Figure 4: FTIR spectrums of commercial, unsintered and sintered HA

3.3 XRD Analysis

The powder X-Ray Diffraction spectrums of commercial, unsintered and sintered HA are shown in Figure 5. These XRD measurements have clearly showed that crystallinity has increased when the hydroxyapatite was sintered at 800°C (Murugan *et at*., 2005). It shows very similar structure with the commercial HA. In all the spectra, a cluster of very sharp XRD peaks are found at 2θ of 32°-34° having more similar peaks for commercial and sintered HA.

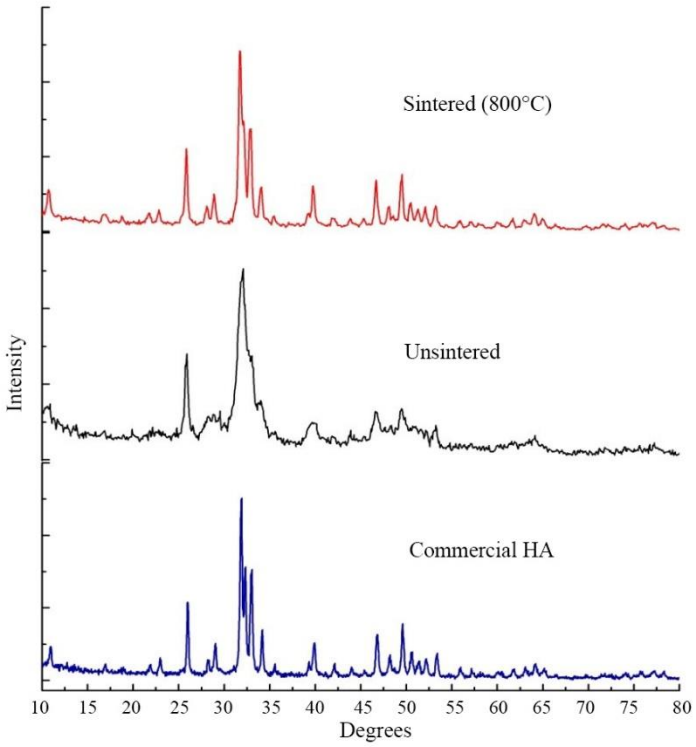

Figure 5: The XRD patterns of commercial, unsintered and sintered HA

3.4 Particle Size Analysis

Particle size of sintered HA was analyzed and found that the average particle size was 1518 nm. Figure 6 shows the graph of particle size distribution of sintered HA.

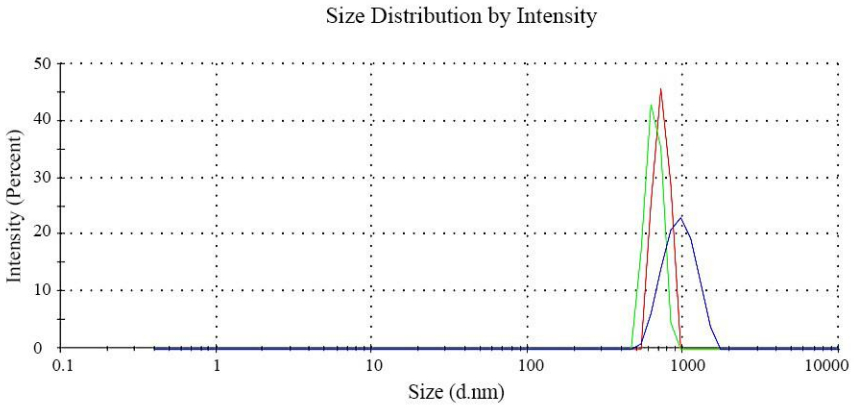

Figure 6: The graph of size distribution by intensity

The particle size gets increased after the sintering as the solid particles get fused at the elevated temperature. It has been recorded that the water-uptake and elution values of materials filled with nano-HA were higher than those of materials filled with micro-HA (Rodríguez *et al*., 2019). Nano-size particles have a large interface for interaction with the matrix, but they also have a high surface-excess energy. When nano-HA was used as reinforcing filler, the high repulsion forces generated in the interface leads to the formation of agglomerates which were heterogeneous. Further they have found that the mesoporous agglomerates formed by the HA nanoparticles had a highly hygroscopic nature and retained adsorbed water (Saghiri *et al*., 2015). Therefor the particle size of the HA filler obtained in the study is ideal for the zinc phosphate dental cement since a dental filling material should have very low water-up take and elution properties.

3.5 Mechanical Characterization

Mechanical properties of a dental filling material are very crucial because it is directly affect the grinding function of the filled tooth. This is a particle reinforced composite material where HA filler (dispersed phase) is dispersed in zinc phosphate matrix (continuous phase). Several factors such as properties and relative amounts of the constituent phase and geometry of the dispersed phase (shape, size, distribution and concentration) affect the mechanical properties of a composite. Strength depends on the strong bonding of the particle-matrix interface (Suh *et al*., 2009). These reinforcing particles tend to restrain movement of the matrix phase in the vicinity of each particle. In essence, the matrix transfers some of the applied stress to the particles, which bear a fraction of the load. The degree of reinforcement or improvement of mechanical behavior depends on strong bonding at the matrix–particle interface (Belli *et al*., 2014).

When the powder mixture is mixed with the liquid mixture an exothermic acid base reaction is taken place and as a result, hard cement is formed. The reaction is as follows.

$$3ZnO + 2\ H_3PO_4 + H_2O \rightarrow Zn_3(PO_4)_2.4H_2O \qquad 2$$

Phosphoric acid attacks the surface of the particles and release Zn ions into the reaction medium. Aluminum forms complexes with phosphoric acid forming zinc alumino phosphate gel. This cementation process and handling time is affected by powder/ liquid ratio and particle size (Jabri *et al*., 2012). When particle size is decreasing setting time also decreases (faster cementation). However, small particle size causes handling difficulties.

Table 6: The values obtained for CS and DTS

Test \ HA wt%	0%	1%	2%	5%	10%	20%	50%
Compressive Strength (CS)	43.24	43.36	48.34	59.32	66.85	61.35	44.22
Diametral Tensile strength (DTS)	11.88	10.5	12.12	12.64	18.88	13.53	12.56

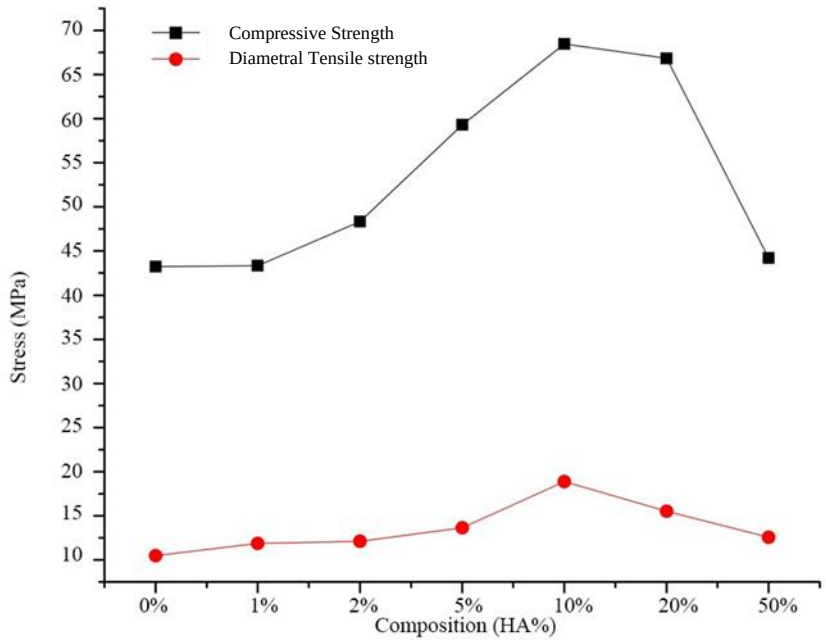

Figure 7: The graphical representation of CS and DTS

The values obtained for the CS and DTS are shown in Figure 7 and extracted numbers are included in the Table 6. According the results, CS has gradually increased with the increasing of filler percentage reaching its maximum value of 66.85 MPa at 10% and decreases slowly. Previous study showed that CS of zinc phosphate dental cement is in the range of 50 – 110 MPa and DTS is around 5.5 MPa (Fleming *et al*., 1999).

With increase of the filler volume the working time also increases which led to a homogeneous mixture with minimizing of voids and heterogeneous agglomerates. Voids initiate the cracks and their propagation which ultimately cause the material failure (Hilfi *et al*., 2019). This is due to the reduction of ZnO amount to react with phosphoric acid. A similar pattern was also observed for the DTS values showing the highest value (18.88 MPa) at 10% of HA. This is because HA added Zinc Phosphate cement has a lower Diametral Tensile Strength than Compressive strength because ceramics are great at bearing compression but weak under tension.

3.6 Elution Test

Table 7 and Figure 8 bellow show the numerical and graphical representation of the data obtained in elution test respectively. When the HA filler ratio is increased the elution, percentage has gradually decreased up to 10% and has then increased. The similar behavior is observed for both aqueous lactic acid solutions of pH 3 and 5. However, acid solutions show higher values compared to water (pH 7).

Table 7: Values obtained from elution test

Test \ HA wt %	0%	1%	2%	5%	10%	20%	50%
Water (P^H 7)	7.9605	7.1915	5.2742	3.8266	2.4159	6.1520	9.5307
Lactic acid (P^H 5)	8.9050	7.6118	6.2440	4.6427	3.0377	6.5540	10.0987
Lactic acid (P^H 3)	9.6721	8.8746	7.0197	5.0578	3.8915	6.8050	11.1765

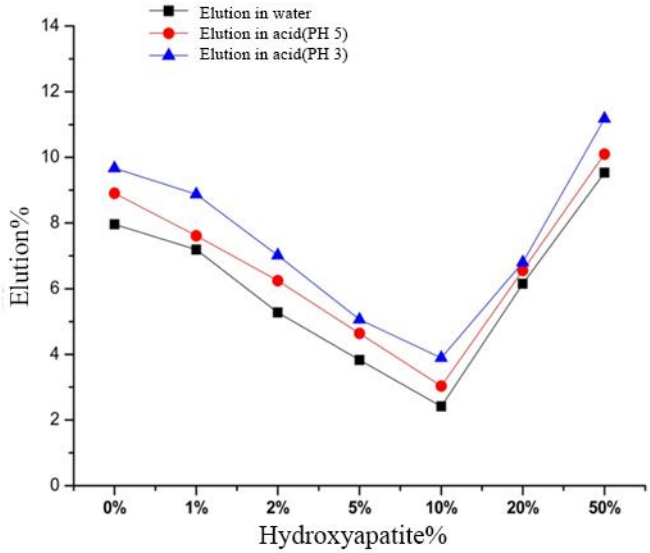

Figure 8: The graphical representation of data obtained in elution test

Having a relatively lower elution percentage with 10% HA is highly favorable for the durability of the dental fillings inside the oral cavity. In generally, there are considerable pH and temperature fluctuations due the food we consume inside the oral cavity. The enamel starts to degrade when pH value drops below 5.5 (Piwowarczyk and Lauer *et al*., 2003). Dental plaque is naturally formed on the surface of the enamel by bacteria that ferment the remaining sugar molecules on the surface of the teeth. They produce lactic acid that causes the enamel degradation. In our results, it showed that developed dental filling has also better resistance against acid elution.

4. Conclusions

Finally, it can be concluded that there is a possibility to incorporate Hydroxyapatite synthesized from *Crassostrea madrasensis* oyster shells into Zinc Phosphate dental cement. The XRD and XRF analysis of synthesized HA showed more similar structure and chemical composition respectively with the commercial HA. Our FTIR results of synthesized HA confirmed that the availability of characteristic vibrational modes related to the structure of $Ca_5(PO_4)_3(OH)_2$. Among prepared different compositions, composite having 10% HA has showed better mechanical properties and lowest elution percentage in all three solutions.

5. References

Abdulrahman, I., Tijani, H.I., Mohammed, B.A., Saidu, H., Yusuf, H., Ndejiko, J.M. and Mohammed, S., (2014). From garbage to biomaterials: an overview on egg shell-based hydroxyapatite. *Journal of Materials*, 802467.

Belli, R., Kreppel, S., Petschelt, A., Hornberger, H., Boccaccini, A.R. and Lohbauer, U., (2014). Strengthening of dental adhesives via particle reinforcement. *Journal of the mechanical Behavior of Biomedical Materials*, 37, 100-108.

Berzina-Cimdina, L. and Borodajenko, N., (2012). Research of calcium phosphates using Fourier transform infrared spectroscopy. *Infrared Spectroscopy-Materials Science, Engineering and Technology*, 12, 251-263.

Cariou, E., Guivel, C., La, C., Lenta, L. and Elliot, M., (2017). Lead accumulation in oyster shells, a potential tool for environmental monitoring. *Marine pollution bulletin*, 125, 19-29.

Fleming, G.J.P., Marquis, P.M. and Shortall, A.C.C., (1999). The influence of clinically induced variability on the distribution of compressive fracture strengths of a hand-mixed zinc phosphate dental cement. *Dental Materials*, 15, 87-97.

Fleming, G.J.P., Shelton, R.M., Landini, G. and Marquis, P.M., (2001). The influence of mixing ratio on the toughening mechanisms of a hand-mixed zinc phosphate dental cement. *Dental Materials*, 17, 14-20.

Hilfi, S.A., AlBadr, R.M. and Ziadan, K.M., (2019). Physical-mechanical properties of dental composites by addition oyster shell powder as fillers. *Basrah Journal of Science*, 37,103-112.

Jabri, M., Mejdoubi, E., El Gadi, M. and Hammouti, B., (2012). Optimization of hardness and setting time of dental zinc phosphate cement using a design of experiments. *Arabian Journal of Chemistry*, 5, 347-351.

Jamarun, N., Azharman, Z., Arief, S., Sari, T.P., Asril, A. and Elfina, S., (2015). Effect of temperature on synthesis of hydroxyapatite from limestone. *Rasayan J. Chem*, 8, 133-137.

Kantharia, N., Naik, S., Apte, S., Kheur, M., Kheur, S. and Kale, B., (2014). Nano-hydroxyapatite and its contemporary applications. *Bone*, 34, 1-71.

Morgan, H., Wilson, R.M., Elliott, J.C., Dowker, S.E.P. and Anderson, P., (2000). Preparation and characterization of monoclinic hydroxyapatite and its precipitated carbonate apatite intermediate. *Biomaterials*, *21*, 617-627.

Murugan, R. and Ramakrishna, S., (2005). Crystallographic study of hydroxyapatite bioceramics derived from various sources. *Crystal Growth & Design*, 5, 111-112.

Piwowarczyk, A. and Lauer, H.C., (2003). Mechanical properties of luting cements after water storage. *Operative dentistry*, 28, 535-542.

Piyathilaka, M.A.P.C., Hettiarachchi, M. and Wanninayake, W.M.T.B., (2012). Growth and health status of cultured edible oyster, *Crassostrea madrasensis* (Preston) in the Panadura estuary, Sri Lanka. *Journal of the National Science Foundation of Sri Lanka*, 40 (3), 201 -210.

Raghukumar, C., Rao, V.P.C. and Iyer, S.D., (1989). Precipitation of iron in windowpane oyster shells by marine shell-boring cyanobacteria. *Geomicrobiology*, 7, 235-244.

Reyes-Gasga, J., Martínez-Piñeiro, E.L., Rodríguez-Álvarez, G., Tiznado-Orozco, G.E., García-García, R. and Brès, E.F., (2013). XRD and FTIR crystallinity indices in sound human tooth enamel and synthetic hydroxyapatite. *Materials Science and Engineering: C*, 33, 4568-4574.

Rujitanapanich, S., Kumpapan, P. and Wanjanoi, P., (2014). Synthesis of hydroxyapatite from oyster shell via precipitation. *Energy Procedia*, 56, 112-117.

Saghiri, M.A., Asatourian, A., Orangi, J., Lotfi, M., Soukup, J.W., Garcia-Godoy, F. and Sheibani, N., (2015). Effect of particle size on calcium release and elevation of pH of endodontic cements. *Dental Traumatology*, 31, 196-201.

Suh, Y.S., Joshi, S.P. and Ramesh, K.T., (2009). An enhanced continuum model for size-dependent strengthening and failure of particle-reinforced composites. *Acta Materialia*, 57, 5848-5861.

Venkateswarlu, K., Bose, A.C. and Rameshbabu, N., (2010). X-ray peak broadening studies of nanocrystalline hydroxyapatite by Williamson–Hall analysis. *Physica B: Condensed Matter*, 405, 4256-4261.

Wilcock, C.J., Gentile, P., Hatton, P.V. and Miller, C.A., (2017). Rapid mix preparation of bioinspired nanoscale hydroxyapatite for biomedical applications. *Journal of Visualized Experiments*, 120,55343.

Wu, S.C., Hsu, H.C., Wu, Y.N. and Ho, W.F., (2011). Hydroxyapatite synthesized from oyster shell powders by ball milling and heat treatment. *Materials characterization*, 62, 1180-1187.

Yoon, G.L., Kim, B.T., Kim, B.O. and Han, S.H., (2003). Chemical–mechanical characteristics of crushed oyster-shell. *Waste Management*, 23, 825-834.